



Synthesis of organoboron amide-ester branched derivatives of poly(itaconic anhydride-alt-2-vinyl-1,3-dioxolane) and cancer cells interaction studies

Gülten Özçayan*

Turkish Atomic Energy Authority, Department of Radiation and Accelerator Technologies, 06983 Kahramankazan, Ankara, Turkey, ORCID ID orcid.org/0000-0001-9773-4569

ARTICLE INFO

Article history:

Received 21 January 2019

Received in revised form 19 September 2019

Accepted 29 November 2019

Available online 31 December 2019

Research Article

DOI: [10.30728/boron.515517](https://doi.org/10.30728/boron.515517)

Keywords:

Biopolymers,
Cytotoxicity,
Itaconic anhydride,
Organoboron copolymers,
Vinyl dioxolane.

ABSTRACT

New organoboron amide-ester branched derivatives of poly(itaconic anhydride-alt-2-vinyl-1,3-dioxolane) are synthesized by amidolysis and grafting reactions, respectively. The structure and composition of the synthesized compounds are characterized by FTIR-ATR (Fourier Transform-Infrared-Attenuated Total Reflection) and ^1H (^{13}C) NMR (Nuclear Magnetic Resonance) spectroscopy. These novel functionalized boron containing biopolymers are interacted with HeLa (human cervix carcinoma cell) cancer cells and L929 Fibroblast (normal) cells. Their anticancer properties are investigated using a combination of different biochemical analysis methods. It is found that both the values of the cytotoxicity and necrotic indexes are increased due to organoboron linkage but these indexes of organoboron amide-ester derivative are visibly decreased because of α -Hydroxy- ω -methoxypoly(ethylene oxide) (PEO) biocompatibilization. The results of these studies allow us to utilize PEO branched derivatives of synthesized organoboron copolymers (up to $200 \mu\text{g mL}^{-1}$) as therapeutic potential functional copolymer drugs in cancer chemotherapy and Boron-Neutron Capture Therapy (BNCT).

1. Introduction

Copolymers containing both hydrophilic and hydrophobic group are used in a wide variety biological applications [1]. Anhydrides of unsaturated dicarboxylic acids are strong hydrophilic monomers. If unsaturated dicarboxylic acids and their anhydrides such as maleic, citraconic and itaconic anhydrides are grafted onto polymers, these reactive groups as carbonyl or free carboxylic groups can serve as sites for further functionalization of grafted polymers [2]. Itaconic anhydride (IA) copolymers are strongly amphiphilic molecules. Itaconic anhydride is a monomer obtained from renewable resources. IA can be polymerized or copolymerized with various other monomers by different methods [3,4]. The different reactions (alcoholysis, hydrolysis, amidation) of poly(itaconic anhydride) or its copolymers have been investigated extensively [1,5-6]. These polymers have wide applications. IA containing polymers are used as ionomeric materials, compatibilizers, an "acid hardener" for epoxide resins, photoresist materials for microlithography and etc. [7]. The biocompatible and bioactive nature of IA has been revealed its big potential in biomedical applications. Some derivatives of IA containing polymers have been shown to possess biological activity, especially for antitumor or cancer treatments [4,5-11]. IA as an isostructural analogous of maleic anhydride (MAH)

is also formed alternating copolymers with electron-donor vinyl monomers [3,12]. IA is more reactive than MAH because of its highly reactive tertiary radical. Due to this characteristic, it can easily homopolymerize and copolymerize to form polymers with varying compositions, which allows the formation of many anhydride ring containing polymers [7].

At the same time, the degradable cyclic acetal biomedical polymers have been investigated by many researchers because of less toxic degradation products. Also, biomaterials based upon polyacetals and polyketals have been shown potential in drug delivery applications due to their pH dependent degradation properties [13,16]. Dioxolane is a heterocyclic acetal and 2-vinyl-1,3-dioxolane (VDO) copolymers have not been investigated enough for biomedical applications. But Rzyaev [17] et. al. synthesized novel multifunctional colloidal nanofiber electrolytes by using copolymer of itaconic anhydride with 2-vinyl-1,3-dioxolane.

On the other hand, many studies about boron compounds are increased because of three fundamental characteristics of boron; its electronic characteristic, its nuclear characteristic and its characteristic to react with oxygen at high temperature [18]. Boron compounds have nontoxic, eco-friendly, high thermal and biological resistance [19]. These compounds can act as lewis acids due to the empty p-orbital on the boron

*Corresponding author: gulten.ozcayan@taek.gov.tr

center. This allows them to form coordinate covalent bonds with nucleophiles. Besides, the boron center can be converted from neutral trigonal planar (sp^2) to tetrahedral (sp^3) hybridization under proper physiological conditions thus boron containing compounds have the unique chemical and biological properties. Many studies and data have shown that boron is not a naturally toxic element and play an important role in the design of new drugs [20,21]. Recently, investigations related to synthetic synthesis methods of boron-containing compounds including peptidyl boronates/boronic acids, benzoxaboroles, benzoxaborines, benzodiazaborines, amine carboxyborane and amine cyanoborane derivatives have increased for biological activities [20]. In another different study, synthesized boron compound-loaded PLLGA nanoparticles were investigated their biodistributions in tumor-bearing mice compared to PLGA nanoparticles [22]. Paşa et al. [23,24] synthesized various imine based boronic acid (C=N) compounds, characterized them with various spectral techniques and then shown that these synthesized diverse imine based boronic compounds can be used as anticancer agent, antimicrobial agent and antioxidants in the literature [23,24]. Additionally, many different carborane derivatives have been synthesized in medicinal and material chemistry because of high boron contents, high hydrophobicity and an icosahedral geometry. Dicarba-*closo*-dodecaborane (carborane) demonstrates notable thermal and chemical stability. Recently, derivatives of dicarba-*closo*-dodecaborane containing trimethoxyphenyl, magnetic nanoparticles coated with *m*-carboranylphosphinate and etc have synthesized for use as nuclear receptor ligands, bio-functional compounds, optical materials and cancer agents [25,26].

Moreover, boron containing polymers are an important of materials in the inorganic and organometallic polymer fields [18]. There are many studies about the incorporation of organoboranes into the polymers. These polymers are prepared by either direct polymerization of boron functionalized monomers or functionalization of polymers with boron groups. Boron containing functional polymers have been studied in many fields like their use as supported catalyst, luminescent materials, biological imaging agents, polymeric precursors for high temperature performance materials, supramolecular nanomaterials, drug delivery agents, antibacterial agents, antimicrobial surface-active coatings, chemical sensors, neutron detections etc, [18-52]. Among these literature studies, Kahraman [12] and Rzyaev [48] synthesized novel bioengineering functional organoboron copolymer containing maleic anhydride, dioxolane, boronic acid and PEO groups and showed that the synthesized organoboron copolymers can be utilized as therapeutic agent's functional copolymer drugs. The synthesis of alternating organoboron amide-ester branched derivatives of poly(itaconic anhydride-*alt*-2-vinyl-1,3-dioxolane) copolymer are not

reported yet. These polymers containing boron compound may be useful for Boron Neutron Capture Therapy (BNCT). BNCT has attracted much attention as a selective and noninvasive cancer therapy based on the irradiation of boron-10 (^{10}B), a stable isotope, with low energy (thermal) neutrons [53-54]. Two types of the ^{10}B -compounds, sodium borocaptate (BSH) and *l*-4-dihydroxyboronylphenylalanine (BPA), have been used for clinical trials so far [54]. Many different types of bioactive boron-containing compounds have been investigated as therapeutic agents for BNCT [37,46-47,53-58]. In our previous publications [37,46-47], the design, synthesis, characterization and bioengineering properties of organoboron derivatives of various functional carboxyl/anhydride-containing copolymers, including alternating copolymer of MAH with VDO were reported.

The aim of this work is evaluation of anticancer activities (cytotoxicity, apoptotic and necrotic effects) of the synthesized boron-containing functional bioengineering copolymer [poly(itaconic anhydride-*alt*-2-vinyl-1,3-dioxolane)-poly(IA-*alt*-VDO)] and graft copolymers [2-Amidoethyldiphenylborinate-poly(IA-*alt*-VDO) and 2-Amidoethyldiphenylborinate- α -Hydroxy- ω -methoxypoly(ethylene oxide)-ester-poly(IA-*alt*-VDO)] containing a combination of bioactive sites such as carboxyl and amine groups using various biochemical methods such as immuno cytochemical stainings and light and fluorescence inverted microscopy analyses.

2. Materials and methods

2.1. Materials

2-Vinyl-1,3-dioxolane (Cat. No: 440353) and itaconic anhydride (Cat. No: 259926) were obtained from Aldrich. 2-Aminoethyldiphenyl borinate (Cat. No: 126705) and *N*-Ethyl-*N*-(3-dimethylaminopropyl) carbodiimide hydrochloride (EDAC) (Cat. No: SE6383) as a carboxyl activating agent were purchased from Aldrich-Sigma (Germany). α,α' -Azobisisobutyronitrile (AIBN) (Cat. No: 11630) and α -Hydroxy- ω -methoxypoly(ethylene oxide) ($M_n = 2000 \text{ g.mol}^{-1}$) (Cat. No: 81221) from Fluka were supplied. AIBN as an initiator was purified by recrystallization from anhydrous ethanol. *N,N'*-dimethylformamide (DMF) (Cat. No: 277056) from Aldrich-Sigma, chloroform- d_1 (Cat. No: M3420) from Merck and Dimethyl sulfoxide- d_6 (Cat. No: M3424) from Merck were used. Other solvents and reagents were analytical grade and used without purification.

The FTIR-ATR (cm^{-1}) spectrum of IA monomer was determined at: 3127-2940 (broad) antisym. stretching C-H in $\text{R-CH}=\text{CH}_2$, 1843 (m) sym. band in $\text{R-CH}=\text{CH}_2$, 1763 (s) and 1703 (m) bands for antisymmetrical and symmetrical C=O, 1668 (m) C=C stretching band in $\text{RCH}=\text{CH}_2$, 1408-1385 (m) C-H and scissor vibration bands in $\text{R}_2\text{C}=\text{CH}_2$ group, 1274 (s) and 1227 (m) anhydride C-O-C stretching. The FTIR spectrum [13] (cm^{-1})

of VDO is; 2954-2866 (m) antisym. stretching C-H in R-CH=CH₂, 1434 (m) and 1347 (m) CH₂ and C-H bending in R-CH=CH₂, respectively and 1147-1028 C-O vibration bands.

2-AEPB was purified by recrystallization from anhydrous ethanol: m.p. 193.5°C (by DSC); FTIR-ATR Spectra [13, 37, 46-47] (cm⁻¹): 3284 (vs) and 3220 (s) N-H stretching in NH₂, 3066-2870 (s) C-H stretching, 1611 (vs) NH₂ bending and C=C stretching in phenyl groups, 1491(m) and 1334 (m) B-O band, 1432 (vs) fairly strong, sharp band due to benzene ring vibration in phenyl-boronic acid linkage, 1263-1154 (s) fairly strong, sharp bands due to C-N stretching in C-NH₂, 1061 (vs) N-H bending in NH₂ and 750-710 (s) sharp bands from boron-phenyl linkage; ¹H NMR spectrum [9, 25, 34-35] (δ, ppm), in CHCl₃-d₁: CH₂-O 1.49, CH₂-NH₂ 2.96, and 7.38-7.40 (1H), 7.19-7.24 (2H) and 7.13-7.16 (2H) for protons of p-, o- and m-positions in benzene ring, respectively.

α-Hydroxy-ω-methoxy-PEO (Mn 2000 g.mol⁻¹): ¹H NMR spectrum [13, 37, 46-47] (δ, ppm) in CHCl₃-d₁: CH₂-O 3.75-3.45, OH end group 2.61 and O-CH₃ end group 2.16.

HeLa (human cervix carcinoma cell) cancer cells and L929 Fibroblast normal cells obtained from the tissue culture collection of the SAP Institute (Ankara, Turkey). Cell culture flasks and other plastic material were purchased from Corning (NY, USA). The growth medium, which is Dulbecco Modified Medium (DMEM) without l-glutamine supplemented fetal calf serum (FCS) (Cat. No: 01-101-1A), Trypsin-EDTA (Cat. No: 03-079-1B) were purchased from Biological Industries (Kibbutz Beit Haemek, Israel). The primary antibody and caspase-3 (Cat. No: 3015) was purchased from lab Vision (Germany), cell proliferation reagent WST (Cat. No: 11 644 807 001) (Roche, Germany).

2.2. Synthesis of poly(itaconic anhydride-alt-2-vinyl-1,3-dioxolane)

The copolymerization procedure followed the charge transfer complex (CTC) reaction described by Kahraman et. al. [13,17]. The reaction scheme is shown in Figure 1. IA has a higher reactivity than itaconic acid, but it is easily hydrolyzed by water. In order to retain the anhydride functionality in the copolymer, all the glassware and reactants were used dried before copolymerization.

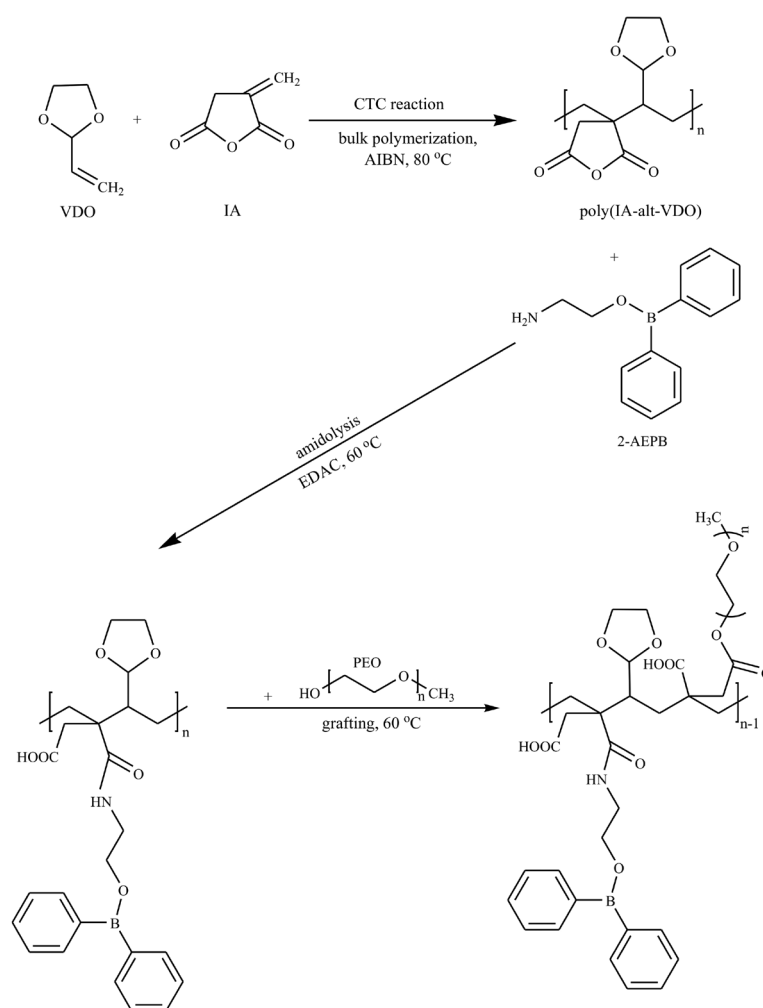


Figure 1. Synthetic pathway of the organoboron amide-ester branched derivatives of alternating copolymer of itaconic anhydride and 2-vinyl-1,3-dioxolane.

Poly(IA-*alt*-VDO) copolymer was synthesized by bulk polymerization technique. Appropriate quantities of liquid IA as a mole ratios of VDO: IA= 1:1 were dissolved in liquid VDO with AIBN initiator (AIBN= 1.0 wt. %) at 80 °C in a round-bottom flask equipped with a magnetic stir bar and a condenser under a nitrogen atmosphere. The reactions were carried out at 80 °C and stirred continuously overnight. After the polymerizations were completed, the reaction solution was precipitated in diethyl ether at ambient temperature and dried at 60 °C in a vacuum oven. The poly(IA-*alt*-VDO) copolymer was characterized by FTIR, ¹H NMR and ¹³C NMR spectra.

2.3. Synthesis of 2-amidoethyldiphenylborinate-poly(IA-*alt*-VDO)

To synthesize 2-Amidoethyldiphenylborinate-poly(IA-*alt*-VDO) [poly(IA-*alt*-VDO)-*g*-AEPB] at different [copolymer]/[2-AEPB] molar ratios by using amidolysis reaction, the reaction was carried out in *N,N*-dimethylformamide (DMF) at 60 °C with EDAC catalyst under a nitrogen atmosphere. Reaction conditions: [2-AEPB]= 0.066 mol.l⁻¹, mole ratios of [(IA-*alt*-VDO)/(2-AEPB)]= 1:1, 2:1, 4:1 and EDAC= 1.0 wt. %. A mixer, temperature control unit and condenser were used. An appropriate quantity of poly(IA-*alt*-VDO) copolymer dissolved in DMF and then 2-AEPB and EDAC were added in a standard pyrex-glass reactors. The reaction mixture was flushed with dried nitrogen gas for 5 min, then sealed and placed in a thermo stated silicon oil bath at 60 °C to intensive mixing for 5 h. The synthesized organoboron amide copolymer was precipitated with diethyl ether, filtered from reaction media and dried at 40 °C under vacuum. The organoboron amide copolymer was characterized by FTIR, ¹H NMR and ¹³C NMR spectra.

2.4. Synthesis of 2-Amidoethyldiphenylborinate-PEO-ester-poly(IA-*alt*-VDO)

The esterification (grafting) of organoboron amide polymer with PEO ($M_n = 2000 \text{ g.mol}^{-1}$) was carried out in DMF at 60 °C for 1 h. Organoboron amide polymer in mole ratio of [(IA-*alt*-VDO) / (2-AEPB)] = 2:1 was used. The ratio of the organoboron linkages of organoboron amide polymer was 19.24 mol % and polymer / PEO feed molar ratio was at (1/ 0.01). PEO branched copolymer [poly(IA-*alt*-VDO)-*g*-AEPB-*g*-PEO] was isolated from reaction mixture by precipitation with diethyl ether and dried 40 °C under vacuum. The ¹H NMR and ¹³C NMR spectra were used for characterization.

Synthetic partway of the side-chain amide-ester-carboxyl functionalized organoboron poly(IA-*alt*-VDO) copolymers can be represented in Figure 1.

2.5. Characterization

Fourier transform infrared (FTIR-ATR) spectroscopy was used to determine the copolymer compositions with FTIR Nicolet 8700 spectrometer in the 3700–600 cm⁻¹

range. ¹H and ¹³C NMR spectra were performed on a Bruker Avance (300 MHz) spectrometer with DMSO-*d*₆ as a solvent at 25 °C.

2.6. Cytotoxicity

HeLa and L929 Fibroblast (50/10⁻³ cells.well⁻¹) cells were placed in DMEM by using 96-well plates for WST cytotoxicity's experiments. Different amounts of copolymers poly(IA-*alt*-VDO), poly(IA-*alt*-VDO)-*g*-AEPB, poly(IA-*alt*-VDO)-*g*-AEPB-*g*-PEO (about 0-250 µg.mL⁻¹ in aqueous solutions) were put into wells containing cells, respectively. Plate known as control group only includes medium (MO abs, maximum viability). The plates were kept in the CO₂ incubator (37 °C in 5% CO₂) for 72 h and then the medium was replaced with fresh medium. Following this incubation, WST reagent (25 µL) was added into each well, and the cells were cultured for further 4 h incubation. After that, plates were read as absorbance value in Elisa Microplate Reader at 440 nm and reference wave length at 440 nm. While living cells are seen dark blue, there is no color in dead cells. Medium containing hydrogen peroxide was used as negative control (MI abs, minimum viability). The number of living and dead cells were counted with a haemocytometer (C.A. Hausse & Son Phluila, USA), using lighth microscope at ×200 magnification. Percentage of cell viability was obtained from % inhibition formula $\{[1 - (\text{Test abs} - \text{MO abs}) / (\text{MO abs} - \text{MI abs})] \times 100\}$. The value obtained from here was subtracted from 100, to make % cell viability.

2.7. Analysis of apoptotic and necrotic cells

An analysis of apoptotic and necrotic cells was performed by double staining method to quantify the number of apoptotic cells in culture on basis of scoring of apoptotic cell nuclei. HeLa and L929 Fibroblast cells were placed in DMEM by using 24-well plates. After treating with different amount functional polymers (about 0-200 µg.mL⁻¹ in aqueous solutions) for 24 hour period, both attached and detached cells were collected. Double staining solution [RNase, Hoechst dye, propidium iodide (PI)] was added to the cells and incubated for 20 min. Then, 10-50 mL of cell suspension was smeared on slide and coverslip for examination by fluorescence microscopy with DAPI and FITC (480-520 nm) filters. The nuclei of normal cells were stained light blue but apoptotic cells were stained dark blue by the Hoechst dye.

The apoptotic cells were identified by their nuclear morphology as a nuclear fragmentation or chromatin condensation. Necrotic cells were staining red by PI. Necrotic cells lacking plasma membrane integrity and PI dye cross cell membrane, but PI dye don't cross non necrotic cell membrane. Ten apoptotic and necrotic cells in microscopic field were randomly chosen and counted and the result (the apoptotic/necrotic index value) was expressed as a ratio of apoptotic and necrotic cells to normal cells.

The number of apoptotic and necrotic cells were determined by Fluorescence Inverted Microscope (Olympus IX70, Japan). The cell images were also recorded using the light and Fluorescence Inverted microscopes.

2.8. Immune staining method

The other analysis method of apoptotic detection was immunocytochemical stains method. For immunocytochemical stains, cells ($25/10^3$ cells.well⁻¹) were placed in DMEM by using 24-well plates and the plates were kept in the CO₂ incubator (37 °C in 5% CO₂). Then, different amounts of copolymers (about 50-200 mg.mL⁻¹ in aqueous solutions) were put into wells containing cells. After a while, the cells were collected in Falcon tube. Following this procedure, wells were rinsed with phosphate buffered saline, PSB (1 mL) twice and added to trypsin-EDTA (250 mL). Thus, the rest cells were accumulated in the same tube. After centrifugation, aspiration was applied and then pellet was formed with PBS. Cytospin preparations were fixed in 70% formalin for immunocytochemistry. For an indirect immunocytochemical procedure, cytology specimens were treated with 0.2% TritonX100 and then rinsed with 8% BSA dissolved in PBS. After aspiration of BPA, the 100 mL primary antibody [caspase-3 (lab Vision) used at 1:300 dilution] was added and incubated for 1 h at cold temperature. For the secondary antibody application, biotinylated secondary antibody solution (100 mL) incubated for 15 min. Each slide was rinsed with PBS, twice and aspired. By using Streptavidin HRP, the same procedure was applied for each slide. The cells were incubated with DAB solution (Diaminobenzidine from Dako) and hematoxylin, respectively. Diaminobenzidine served as the chromagen and Mayer's

hematoxylin as the counter stain. The immunocytochemical staining results were reviewed independently and blindly by observer without the knowledge of treatment. The immunoreactivity of the caspase-3 antibody is confined to the cytoplasm of apoptotic cells. I counted the number of caspase-3-positive cytoplasmic staining cells in all fields found at ×400 final magnification. For each image, three randomly selected microscopic fields were observed, and at least 100 cells field⁻¹ were evaluated.

3. Results and discussion

3.1. Structure of organoboron derivatives of poly(IA-*alt*-VDO)

VDO monomer as cyclic analogue of alkyl vinyl ethers copolymerized with IA through formation of a charge transfer complex (CTP). Rzyaev et. al. [13] proved that the copolymerization of an electron donor (VDO) with an electron acceptor (MA) monomer goes by formation of a CTP. IA has been mentioned as an alternative to MAH because of the chemical similarity to MAH.

The structures of synthesized copolymers, organoboron copolymers and their PEO branches were confirmed by FTIR-ATR and ¹H (¹³C) NMR analysis.

The copolymerization reaction was determined by FTIR analysis. The FTIR spectra and absorption bands of the VDO, IA and poly(IA-*alt*-VDO) copolymer were shown in Figure 2. The absorptions for the IA were at 1763 and 1703 cm⁻¹ (C=O symmetric and asymmetric stretching of the anhydride unit), 1668 cm⁻¹ (C=C stretching) and 1408 cm⁻¹ (=CH₂ in plane deformation), and for VDO at 1434 cm⁻¹ (CH₂)

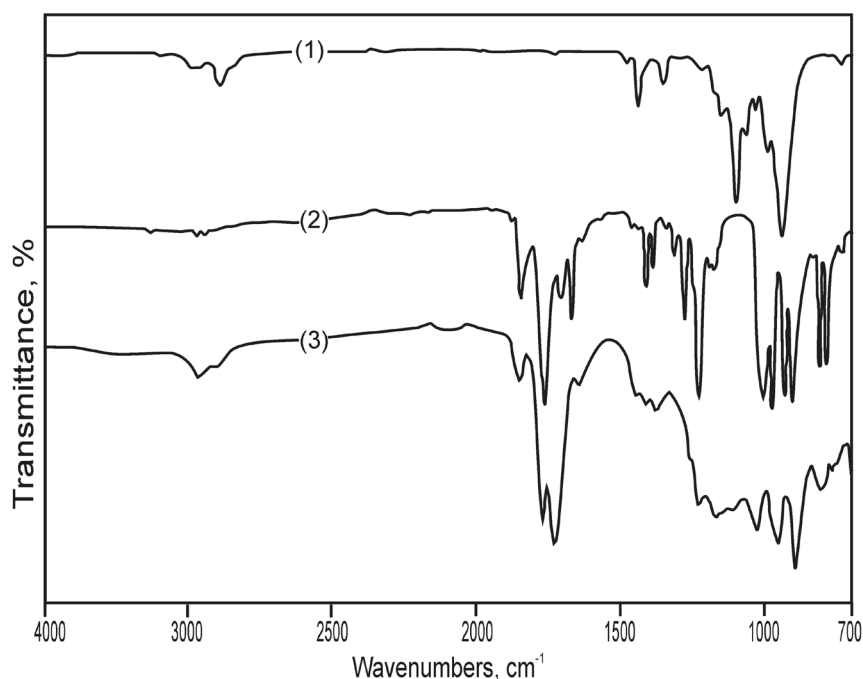


Figure 2. FTIR spectra of (1) VDO (2) IA and (3) poly(IA-*alt*-VDO) copolymer.

and 1347 cm^{-1} (C=C or C-H bending in vinyl group). For the poly(IA-*alt*-VDO) copolymer, the absorption bands associated with C=C stretching bands of vinylene and vinyl groups of IA and VDO monomers (around $1668\text{--}1347\text{ cm}^{-1}$) disappeared in FTIR-ATR spectrum of copolymer, confirming the polymerization. The peaks for the anhydride ring vibrations in the copolymer were at 1768 and 1725 cm^{-1} and the carbonyl stretching of the VDO moved to $1228\text{--}1166\text{ cm}^{-1}$. The anhydride peaks indicate that the anhydride remained intact in the copolymer.

The VDO and IA's characteristic proton and carbon peaks were determined in NMR spectrum of synthesized poly(IA-*alt*-VDO) copolymer as previously mentioned in Rzyaev's study [17]. The characteristic proton peaks of VDO were observed OCH_2 and CH peaks at $6.0\text{--}5.7\text{ ppm}$ and 4.15 ppm in the ^1H NMR spectra of

poly(IA-*alt*-VDO), respectively. COOH broad peak with lowering intensity between 12 and 13 ppm related to trace of hydrolyzation of unhydrated groups under air atmosphere. In the ^{13}C NMR spectrum of poly(IA-*alt*-VDO), characteristic carbon peaks of IA and VDO were also observed at $170\text{--}166\text{ ppm}$ for anhydride C=O and $65\text{--}62\text{ ppm}$ for O-CH_2 in dioxolane ring, respectively.

Comparative spectrum analyzes (Figure 3) of 2-AEPB, poly(IA-*alt*-VDO) and its organoboron derivative indicated that the characteristic bands of anhydride C=O groups disappeared in the spectra of poly(IA-*alt*-VDO)-*g*-AEPB polymer prepared from equimolar feed ratio of copolymer and 2-AEPB. The formation of amide group in this organoboron copolymer was confirmed by the appearance of new bands such as 1737 cm^{-1} (amide I. band), 1650 and 1558 cm^{-1} (amide II. band), 1434 and 1367 cm^{-1} (amide III. band) (Figure 3 and Table 1).

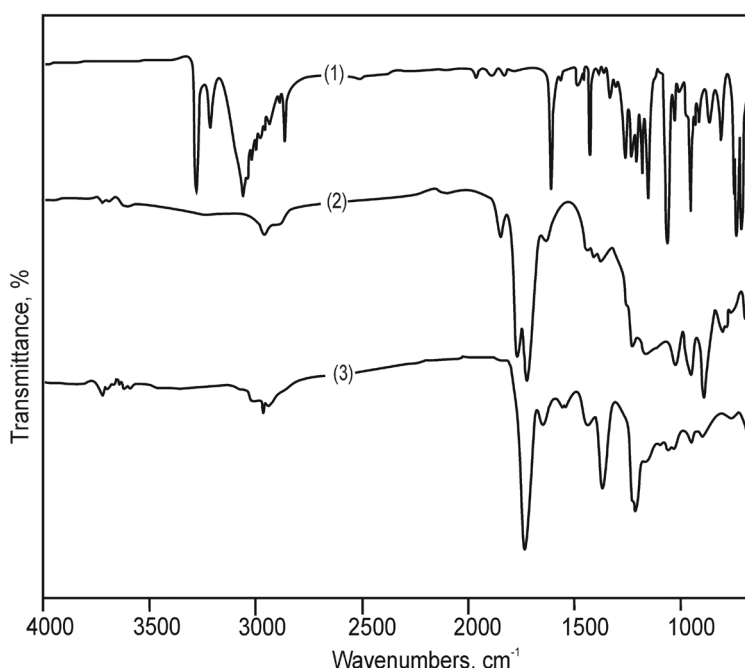


Figure 3. FTIR spectra of (1) 2-AEPB (2) poly(IA-*alt*-VDO) and (3) poly(IA-*alt*-VDO)-*g*-AEPB organoboron copolymer.

Table 1. Absorption bands of poly(IA-*alt*-VDO)-*g*-AEPB organoboron copolymer in FTIR analysis.

Absorption band, cm^{-1}	Band assignments
2-AEPB unit	
3284 (vs), 3220 (s)	N-H stretching in NH_2
3066-2870 (s)	C-H stretching
1611 (vs)	NH_2 bending and C=C stretching in phenyl groups
1491(m), 1334 (m)	B-O band
1432 (vs)	benzene ring vibration
1263-1154 (s)	C-N stretching in C- NH_2
1061 (vs)	N-H bending in NH_2
750-710 (s)	boron-phenyl linkage
poly(IA-<i>alt</i>-VDO)	
2963 (w)	CH stretching band (backbone)
1768 (w), 1725 (m)	C=O in IA unit
1228 (w-m), 1166 (m, broad)	C-O-C stretching in anhydride
poly(IA-<i>alt</i>-VDO)-<i>g</i>-AEPB	
1737 (vs)	C=O stretching (amide I. band)
1650 (m), 1558 (m, broad)	N-H deformation (amide II. band)
1434(w), 1367(m)	C-N stretching (amide III. band)

When 2-AEPB compound was bounded to poly(*IA-alt-VDO*) copolymer via amidolysis reaction, the formation of H-bonded amide linkages in this organoboron polymer was confirmed by a presence of characteristic peaks at 5.8 and 162 ppm in the ^1H NMR and ^{13}C NMR spectra of poly(*IA-alt-VDO*)-*g*-AEPB, respectively (Figure 4). Also, the presence of characteristic proton peaks of organoboron linkages were observed as quarter phenyl peak at 7.2 ppm, triplet B-O-CH₂ peak at 3.35 ppm and quarter NH-CH₂ peak at 2.75 ppm [Figure 4(a)] and it could be said that 2-AEPB was covalently bound to anhydride units. The characteristic carbon resonances from organoboron fragment (C=O of amide

and carboxylic groups 162, CH= in phenyl groups around 128-126 ppm, NH-CH₂ 41 and 42 ppm, CH₂-O 36 and 31 ppm) were also seen in the ^{13}C NMR spectrum of poly(*IA-alt-VDO*)-*g*-AEPB polymer [Figure 4(b)].

The observed proton signals of side-chain PEO branches at 3.4 ppm for CH₂CH₂ unit and 2.57 ppm for OCH₃ end group in the ^1H NMR spectrum of PEO grafted organoboron copolymer [poly(*IA-alt-VDO*)-*g*-AEPB-*g*-PEO] confirmed the esterification of organoboron amide polymer with PEO [Figure 5(a)]. Also, the observed characteristic carbon atom resonances (69.5 ppm for CH₂CH₂ in PEO branch, 62.5 ppm for

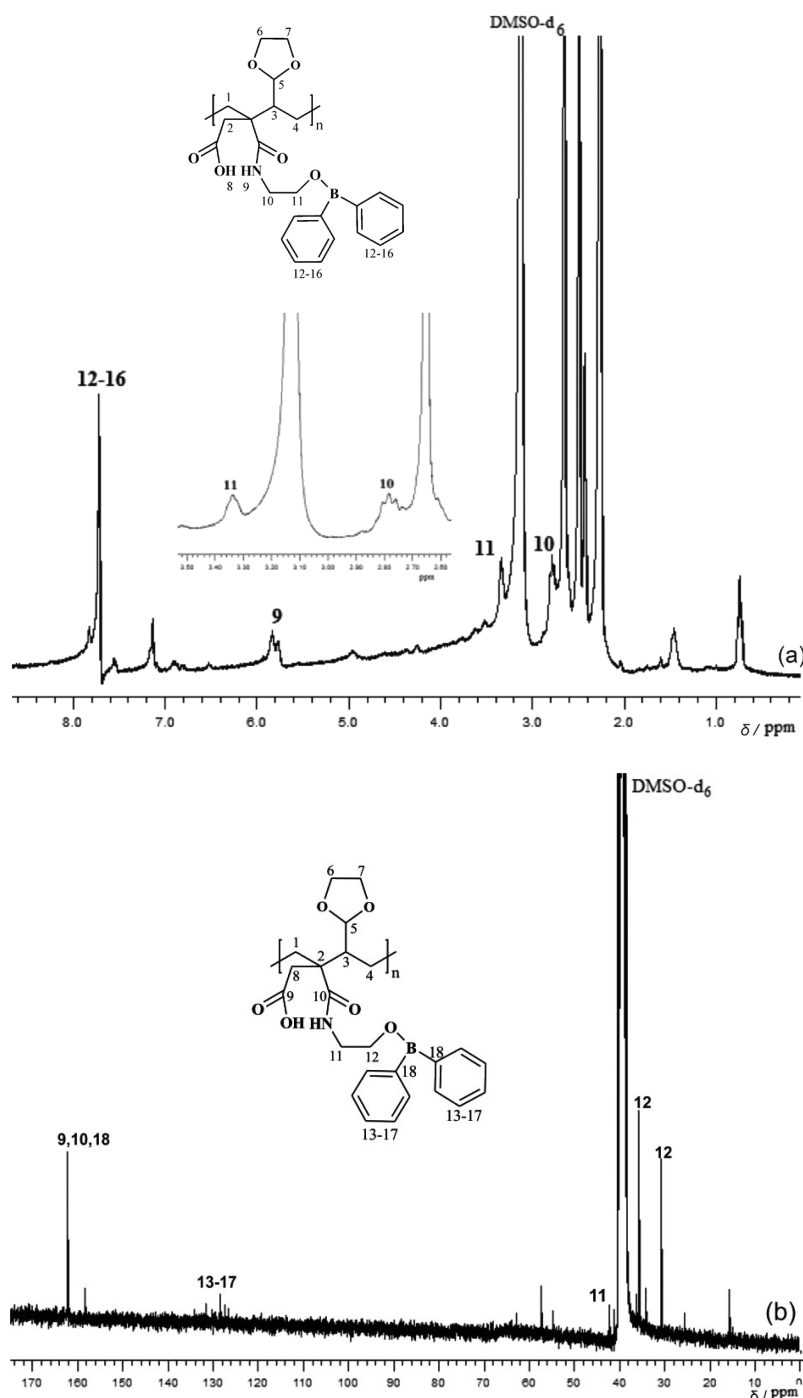


Figure 4. (a) ^1H NMR and (b) ^{13}C NMR spectra of poly(*IA-alt-VDO*)-*g*-AEPB in DMSO-*d*₆.

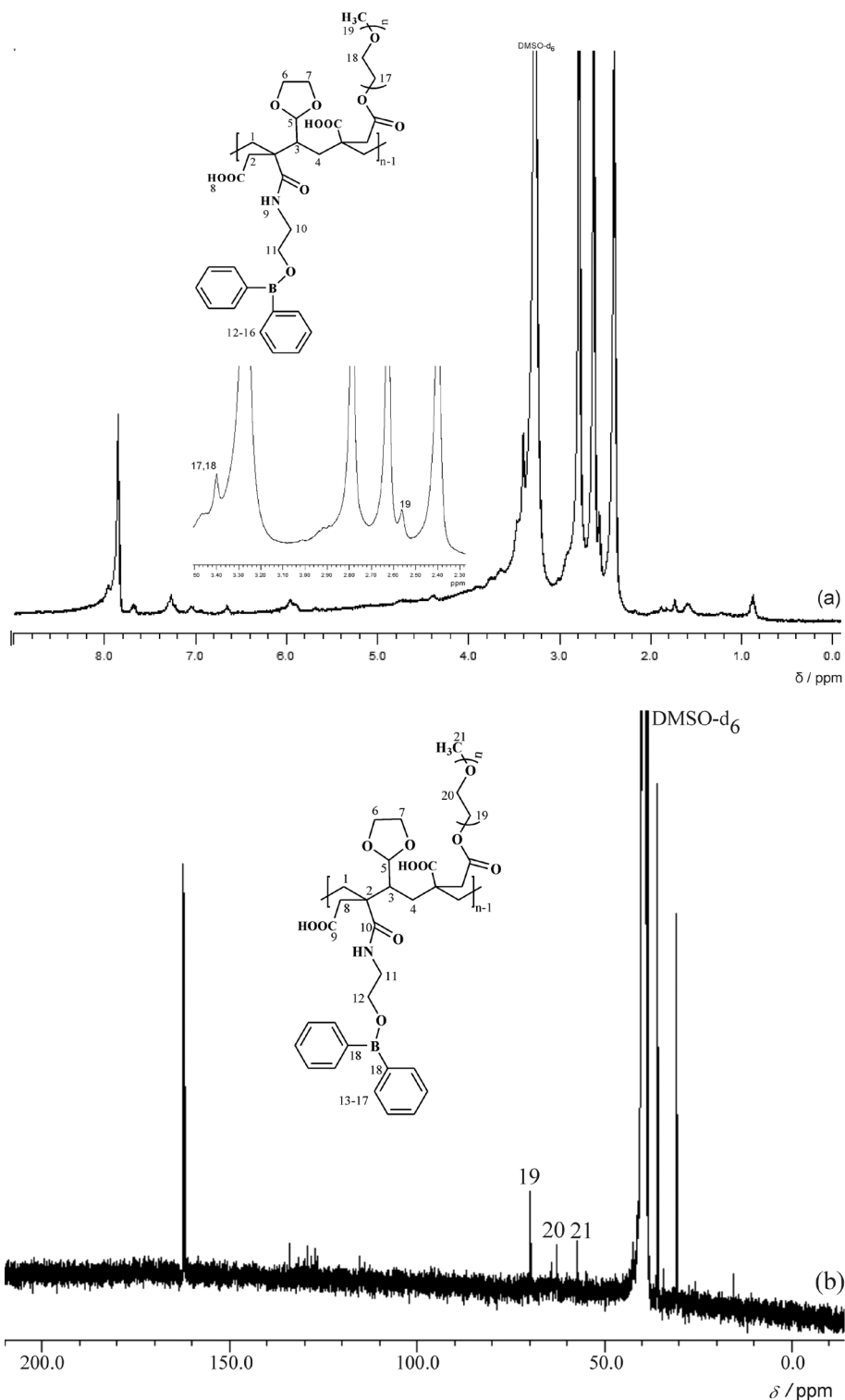


Figure 5. (a) ^1H NMR and (b) ^{13}C NMR spectra of poly(IA-*alt*-VDO)-*g*-AEPB-*g*-PEO in $\text{DMSO-}d_6$.

O-CH₂ and 57.2 ppm for OCH₃ end group) in the ^{13}C NMR spectrum of [poly(IA-*alt*-VDO)-*g*-AEPB-*g*-PEO] [Figure 5(b)] show that the side-chain macrobranched PEO linkages formed.

3.2. Cytotoxicity of poly(IA-*alt*-VDO) and its boron containing and PEO branched derivatives

The obtained cytotoxicity results of the pristine alternating copolymer [poly(IA-*alt*-VDO)] and its organo-

boron amide [poly(IA-*alt*-VDO)-*g*-AEPB] and organo-boron amide-ester [poly(IA-*alt*-VDO)-*g*-AEPB-*g*-PEO] derivatives on HeLa and L929 Fibroblast cells using a WST method were shown in Figure 6.

As seen from plots of concentration of polymers versus percent of cell viability, it was shown that the toxicity of copolymers against cancer cells and normal cells increased with increasing in polymer concentrations between 0 and 250 $\mu\text{g mL}^{-1}$ for 24 h incubation at 37 °C.

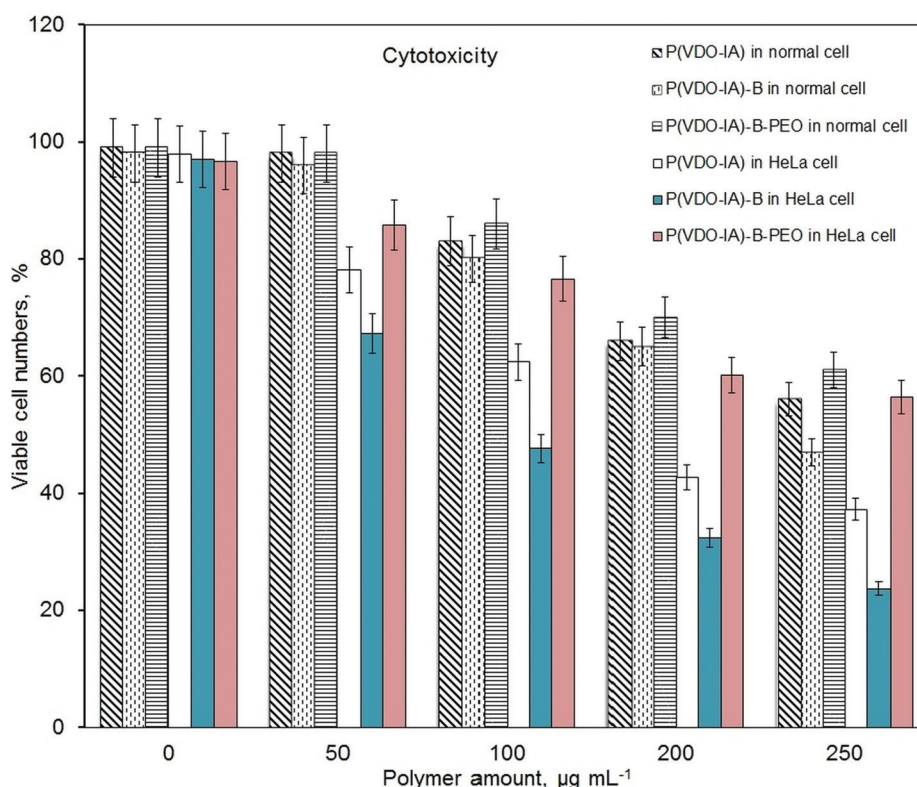


Figure 6. In vitro cytotoxicity of pristine *alternating* copolymer and its organoboron and PEO functionalized derivatives with different amount in a well at 72 h incubation for L929 Fibroblast cells and HeLa cells, respectively. Results are presented as means \pm S.D.

The toxicity of boron containing copolymer [poly(IA-*alt*-VDO)-*g*-AEPB] was more significant than pristine copolymer. Figure shows that the number of viable cells was above 96% for L929 Fibroblast cells and 67% for HeLa cells after incubation of the cells with poly(IA-*alt*-VDO)-*g*-AEPB at concentrations around 50 mg mL⁻¹ for 24 h incubating time in cancer cells and normal cells culture media, respectively. The number of viable cells was also around 80-65% for L929 Fibroblast cells and 50-30% for HeLa in the range of 100-200 µg mL⁻¹ concentration. The cytotoxicity was increased because of organoboron linkage, hydrogen bonding, free carboxylic groups that are form of partial amidolysis of anhydride of pristine copolymer, whole hydrolysis of free anhydride units in the positive charged physiological condition [13,37, 46-48]. The cytotoxicity of PEO containing organoboron copolymer was lower than the one without PEO at 50-250 µg mL⁻¹ concentrations. As it has shown in previous literature studies [13,37,46-48] PEO was bound to organoboron copolymer, the cytotoxicity of organoboron amide-ester [Poly(IA-*alt*-VDO)-*g*-AEPB-*g*-PEO] derivative was decreased because of PEO biocompatibilization (it includes -OH end group and it has long chain structure) Also, the content of organoboron bond in boron containing copolymer was higher than organoboron amide-ester derivative. The poly(IA-*alt*-VDO) and its derivatives had a higher toxicity for cancer cells than normal cells. Viable cell ratio (%) at 200 µg mL⁻¹ polymer concentration in cancer cells was 42.6 \pm 5% [poly(IA-*alt*-VDO)], 32.3 \pm 3% [Poly(IA-*alt*-VDO)-*g*-AEPB] and 60.1 \pm 5%

[Poly(IA-*alt*-VDO)-*g*-AEPB-*g*-PEO], respectively. PEO containing organoboron copolymer is used as therapeutic agent up to 200 µg mL⁻¹ polymer concentration.

3.3. Double staining and Caspase 3 immunostaining results

The destruction process of supramacromolecular structure of cancer cell biomacromolecules could be influenced by the conjugation of copolymer with DNA biomacromolecules of cancer cell through cells/ionized amide and organoboron groups (-H₂N...HOOC-) and H-bondings (O in ether...HOOC-) for this reason, can be exhibited apoptotic and necrotic effects [13,37,46-48].

Apoptotic and necrotic indexes in normal cells and cancer cells were obtained by both double staining and caspase 3 immunostaining methods. Obtained results were summarized in Table 2 and Table 3. When the cells were treated by poly(IA-*alt*-VDO)-*g*-AEPB at 200 µg mL⁻¹ concentrations, the number of apoptotic cells were relatively high in cancer cells and normal cells. The maximum apoptotic index was obtained as 27% from poly(IA-*alt*-VDO)-*g*-AEPB copolymer at 200 µg mL⁻¹ in cancer cells. The number of apoptotic cells for the PEO-containing branched polymers was decreased for HeLa and Fibroblast cells because of PEO biocompatibility. The apoptotic index in cancer cells was higher than that in normal cells at chosen polymer concentration at 24 hours incubation.

Table 2. The comparative analysis of apoptotic and necrotic Fibroblast cell indexes for (I) poly(IA-*alt*-VDO), (II) poly(IA-*alt*-VDO)-*g*-AEPB and (III) poly(IA-*alt*-VDO)-*g*-AEPB-*g*-PEO at 24 hours incubation. Results are presented as means ± S.D.

Polymer concentration ($\mu\text{g}\cdot\text{ml}^{-1}$)	Apoptotic Indexes (%)			Necrotic Indexes (%)		
	I	II	III	I	II	III
0	2±1	1±1	2±1	1±1	1±1	2±1
50	3±1	4±1	4±1	4±1	2±1	2±1
100	7±1	10±1	8±1	19±2	22±3	17±2
150	14±2	17±2	16±2	36±3	45±4	30±3
200	14±2	24±3	12±2	49±4	51±4	38±3

Table 3. The comparative analysis of apoptotic and necrotic HeLa cell indexes for (I) poly(IA-*alt*-VDO), (II) poly(IA-*alt*-VDO)-*g*-AEPB and (III) poly(IA-*alt*-VDO)-*g*-AEPB-*g*-PEO at 24 hours incubation. Results are presented as means ±S.D.

Polymer concentration ($\mu\text{g}\cdot\text{ml}^{-1}$)	Apoptotic Indexes (%)			Necrotic Indexes (%)		
	I	II	III	I	II	III
0	2±1	1±1	1±1		2±1	1±1
50	5±1	13±2	11±2	14±2	23±3	10±1
100	10±1	19±2	14±2	20±3	32±3	14±2
150	13±1	24±3	17±2	37±3	48±4	23±2
200	15±2	27±3	22±3	50±4	59±4	29±2

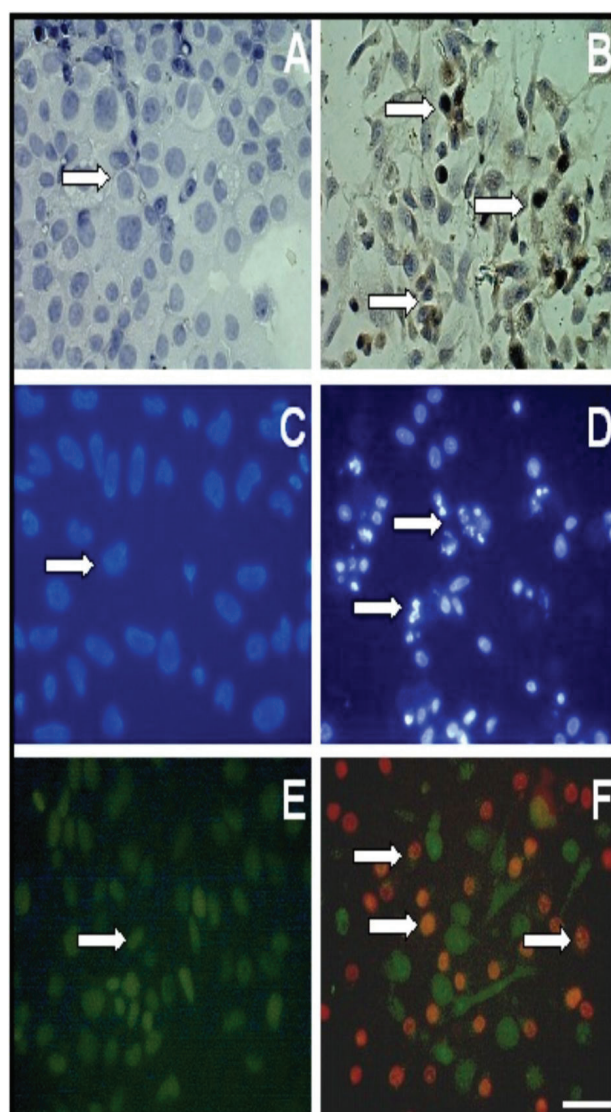


Figure 7. Microscope images: (a) Light microscope images of non-apoptotic HeLa cells as a control group (stained with caspas-3 immunostaining kit) (b) 200 $\mu\text{g}\cdot\text{mL}^{-1}$ concentration of poly(IA-*alt*-VDO)-*g*-AEPB-*g*-PEO/HeLa cells conjugate (stained with caspas-3 immunostaining kit) (c) Fluorescent microscope image of nucleus of untreated HeLa cells as a control (d) nucleus of HeLa cells (stained with Hoechst 33342) incubated with 200 $\mu\text{g}\cdot\text{mL}^{-1}$ concentration of poly(IA-*alt*-VDO)-*g*-AEPB-*g*-PEO (e) Fluorescent microscope image of nucleus of untreated HeLa cells as a control (f) nucleus of HeLa cells (stained with PI dye) incubated with 200 $\mu\text{g}\cdot\text{mL}^{-1}$ concentration of poly(IA-*alt*-VDO)-*g*-AEPB-*g*-PEO. All images were recorded with x400 magnification. Scale bar is 40 μm .

The results of light and fluorescent microscope investigation of the interaction of organoboron polymers with cancer cells were illustrated in Figure 7. All images were recorded with x400 magnification. Scale bar is 40 μm . As the cytoplasm of apoptotic cells treated with complex were stained brown (arrows show apoptotic cell cytoplasm in Figure 7(b)), the cytoplasm of non-apoptotic cells were not stained brown (Figure 7(a)). The Hoechst fluorescent dye in the double staining solution binds to DNA and gives the blue colored cell nuclei (Figure 7(c)) under the blue fluorescent light. Apoptotic cell nuclei were distinguished from other blue nuclei by their distorted borders and brighter appearance (arrows show apoptotic bodies in Figure 7(d)). Fluorescent microscope image of nucleus of untreated HeLa cells (stained with PI dye) as a control was shown in Figure 7(e) and the nucleus of non-necrotic cells was green color. When HeLa cells were stained with propidium iodide fluorescent dye in double-staining solution, the nuclei of necrotic cells appeared in red color under red and green fluorescent light and this indicates that red spots (arrows show necrotic cell nuclei) indicate nucleus of necrotic cells and green spots indicate nucleus of non-necrotic cells (stained with Hoechst 33342) (Figure 7(f)).

The copolymer has lower necrotic index than boron containing copolymer [poly(IA-*alt*-VDO)-*g*-AEPB] at different polymer concentrations for cancer cells and normal cells. It was observed that the necrotic index for boron containing copolymer at 200 $\mu\text{g mL}^{-1}$ concentration was around 60% in HeLa cells. When the organoboron copolymer containing PEO was incubated to cancer cells, the necrotic index decreased in cancer cells and normal cells (38% and 29%, respectively) (Table 2 and 3). Similar results were reported at synthesized different boron compounds in previous studies [13,37,46-48].

The synthesized novel bioengineering functional organoboron copolymers contain hydrophilic/hydrophobic fragments, ethylene amidodiphenylborinate linkages, long branched PEO segments and free carboxylic groups with an ability to conjugate with cancer biomolecules, especially with HeLa cells.

4. Conclusions

This work presents the synthesis and characterization of copolymer of IA with VDO and its organoboron and PEO functionalized derivatives and investigation of their antitumor activity (cytotoxicity, apoptotic and necrotic effects) toward HeLa and Fibroblast cells by using a combination of various biochemical, statistical and microscopy methods.

2-AEPB organoboron and PEO compounds was bound to poly(IA-*alt*-VDO) copolymer by amidization and grafting reactions, respectively. The chemical structure of organoboron amide-ester branched derivatives

of poly(itaconic anhydride-*alt*-2-vinyl-1,3-dioxolane) was confirmed by FTIR and NMR analyses. The synthesized compounds contain a combination of physically and chemically reactive functional groups as antitumor sites.

It was observed that antitumor activity of these copolymers significantly depends on the structure, amount of ionizable free carboxylic groups, organoboron linkages and complex fragments in the functionalized copolymer. These observations confirmed the realization of apoptosis and necrosis processes in the interaction of organoboron functionalized polymers with HeLa and Fibroblast cells. It was observed that both the cytotoxicity and necrotic indexes of synthesized functional organoboron polymers show approximately the same values. The cytotoxicity of PEO containing organoboron copolymer was lower than that without PEO at lower concentrations. Apoptotic and necrotic indexes of cancer cells were obtained higher than normal cells. The apoptotic and necrotic indexes for boron containing copolymer were relatively higher than other copolymers at 200 $\mu\text{g mL}^{-1}$. The apoptotic and necrotic indexes for the copolymers containing PEO were decreased in cancer cells because of PEO biocompatibility.

The results of these studies allow us to utilize the synthesized organoboron copolymers and their PEO branched derivatives (up to 200 $\mu\text{g mL}^{-1}$) as therapeutic potential functional copolymer drugs in cancer chemotherapy and boron-neutron capture therapy which will be the subject of our future investigations.

Acknowledgements

The author thanks for the support of the TAEK (Turkish Atomic Energy Authority) through TAEK-A3.H2.P2.01 project. Also, the author would like to express my gratitude and appreciation to Prof. Dr. Zakir M. O. Rzayev for the helpful discussions about polymer synthesis and materials characterization and Prof. Dr. Mustafa Türk at Kırıkkale University for his works on experimental cell culture and also fruitful discussions.

References

- [1] Milovanovic M. B., Trifunovic S. S., Katsikas I., Popovic I. G., Preparation and modification of itaconic anhydride-methyl methacrylate copolymers, J. Serb. Chem. Soc., 72 (12), 1507-1514, 2007.
- [2] Devrim Y. G., Rzaev Z. M. O., Pişkin E., Functionalization of isotactic polypropylene with itaconic anhydride, Polym. Bull., 59 (4), 447-456, 2007.
- [3] Drougas J., Guile R. L., Copolymerization of itaconic anhydride and styrene, determination of reactivity ratios, J. Polym. Sci., 55 (161), 297-302, 1961.
- [4] Ishida S., Saito S., Polymerization of itaconic acid derivatives, J. Polym. Sci. A1, 5, 689-705, 1967.
- [5] Shang S., Huang S. J., Weiss R. A., Synthesis and

- characterization of itaconic anhydride and stearyl methacrylate copolymers, *Polymer*, 50 (14), 3119-3127, 2009.
- [6] Papanu V. D., Amide-imide derivatives of homopolymers of itaconic anhydride having antitumor activity, USA patent, Monsanto Co., EP 0070142-A2, 1983.
- [7] Belov N., Reactive fluoropolymers synthesis and application, PhD thesis, Aachen University, Germany, 2011.
- [8] Müller F., Torger B., Allertz P. J., Jähnichen K., Keßler S. et al, Multifunctional crosslinkable itaconic acid copolymers for enzyme immobilization, *Eur. Polym. J.*, 102, 47–55, 2018.
- [9] Li H., Zhang X., Zhang X., Yang B., Wei Y., Stable biocompatible cross-linked fluorescent polymeric nanoparticles based on AIE dye and itaconic anhydride, *Colloid. Surfaces B.*, 121, 347–353, 2014.
- [10] Nayak P. S., Narayana B., Sarojini B. K., Sheik S., Shashidhara K.S., Chandrashekar K.R, Design, synthesis, molecular docking and biological evaluation of imides, pyridazines, and imidazoles derived from itaconic anhydride for potential antioxidant and antimicrobial activities, *J. Taibah Univ. Sci.*, 10, 823–838, 2016.
- [11] Gupta V. K., Sood S., Agarwal S., Saini A. K., Pathania D., Antioxidant activity and controlled drug delivery potential of tragacanth gum-cl-poly (lactic acid-co-itaconic acid) hydrogel, *Int. J. Biol. Macromol.*, 107, 2534–2543, 2018.
- [12] Rzaev Z. M. O., Complex-radical alternating copolymerization, *Prog. Polym. Sci.*, 25, 163-217, 2000.
- [13] Kahraman G., Türk M., Rzaev Z. M. O., Söylemez E. A., Oğuztüzün S., Bioengineering functional copolymers. XX. Synthesis of novel anticancer active poly(maleic anhydride-alt-2-vinyl-1,3-dioxolane) and its organoboron amide-ester branched derivative, *Haceteppe J. Biol. & Chem.*, 40 (2), 183-194, 2012.
- [14] Falco E. E., Patel M., Fisher J. P., Recent developments in cyclic acetal biomaterials for tissue engineering applications, *Pharmaceut. Res.*, 25 (10), 2348-2356, 2008.
- [15] Patel M., Betz M. W., Geibel E., Patel K. J., Caccamese J. F., Coletti D. P., Sauk J. J., Fisher J. P., Cyclic acetal hydroxyapatite nanocomposites for orbital bone regeneration, *Tissue Eng. Pt. A*, 16 (1), 55-65, 2009.
- [16] Shi S., Gao H., Wu G., Nie J., Cyclic acetal as coinitiator for bimolecular photoinitiating systems, *Polymer* 48 (10), 2860–2865, 2007.
- [17] Rzaeva Z. M. O., Şimşek M., Bunyatovac U., Salamov B., Novel colloidal nanofiber semiconductor electrolytes from solution blends of PVA/ODA–MMT, poly (itaconic anhydride-alt-2-vinyl-1,3-dioxolane) and its Ag-carrying polymer complex by reactive electrospinning, *Colloids and Surfaces A: Physicochem. Eng. Aspects*, 492, 26–37, 2016.
- [18] Parab K., Boron containing vinyl aromatic polymers: synthesis, characterization and applications, PhD thesis, The State University of New Jersey, Newark, New Jersey, 2009.
- [19] Donmez Cavdar A., Mengelolu F., Karakus K., Effect of boric acid and borax on mechanical, fire and thermal properties of wood flour filled high density polyethylene composites, *Measurement*, 60, 6–12, 2015.
- [20] Yang F., Mingyan Z., Zhang J., Zhou H., Synthesis of biologically active boron-containing compounds, *Med. Chem. Commun.*, 9, 201-211, 2018.
- [21] Fernandes G.F.S., Denny W.A., Santos J.L.D, Boron in drug design: Recent advances in the development of new therapeutic agents, *Eur. J. Med. Chem.*, 179, 791-804, 2019.
- [22] Takeuchi I., Nomura K., Makino K., Hydrophobic boron compound-loaded poly(L-lactide-co-glycolide) nanoparticles for boron neutron capture therapy, *Colloid. Surfaces B.*, 159, 360–365, 2017. apy, *Adv. Drug Deliver. Rev.*, 26 (2-3), 231-247, 1997.
- [23] Paşa, S., Synthesis and characterization of di-Schiff based boronic structures: Therapeutic investigation against cancer and implementation for antioxidant, *J. Mol. Struct.*, 1195, 198-207, 2019.
- [24] Pasa S., Aydın S., Kalaycı S., Boğa M., Atlan M., Bingul M., Şahin F., Temel H., The synthesis of boronic-imine structured compounds and identification of their anticancer, antimicrobial and antioxidant activities, *J. Pharmaceut. Anal.*, 6, 39–48, 2016.
- [25] Kaise A., Endo Y., Ohta K., Anti-cancer activity of m-carborane-containing trimethoxyphenyl derivatives through tubulin polymerization inhibition, *Bioorg. Med. Chem.*, 27, 1139–1144, 2019.
- [26] Oleshkevich E., Morancho A, Saha A., Galenkamp K.M.O., Grayston A. et al., Combining magnetic nanoparticles and icosahedral boron clusters in biocompatible inorganic nanohybrids for cancer therapy, *Nanomed-Nanotechnol.*, 20, 101986, 2019.
- [27] Cambre J. N., Roy D., Gondi S. R., Sumerlin B. S., Facile strategy to well-defined water-soluble boronic acid (co)polymers, *J Am. Chem. Soc.*, 129, 10348–10349, 2007.
- [28] Camerano J. A., Casado M. A., Ciriano M. A., Oro L. A., Tris(pyrazolyl)borate carbosilane dendrimers and metallodendrimers, *Dalton Trans.*, 44, 5287–5293, 2006.
- [29] Cheng F., Jakle F., Raft polymerization of luminescent boron quinolate monomers, *Chem. Commun.*, 46, 3717–3719, 2010.
- [30] Cheng F., Jakle F., Boron-containing polymers as versatile building blocks for functional nanostructured materials, *Polym. Chem.*, 2 (10), 2122-2132, 2011.
- [31] Cui C., Bonder E. M., Jakle F., Weakly coordinating amphiphilic organoborate block copolymers, *J. Am. Chem. Soc.*, 132, 1810-1812, 2010.
- [32] Cui C., Bonder E. M., Jakle F., Organoboronium amphiphilic block copolymers, *J. Polym. Sci., Part A: Polym. Chem.*, 47 (23), 6612–6618, 2009.
- [33] Deore B. A., Freund M. S., Self-doped polyaniline nanoparticle dispersions based on boronic acid-phosphate complexation, *Macromolecules*, 42, 164-168, 2009.
- [34] Deore B. A., Yu I., Woodmass J., Freund M. S., Con-

- ducting Poly(anilineboronic acid) nanostructures: controlled synthesis and characterization, *Macromol. Chem. Phys.*, 209 (11), 1094-1105, 2010.
- [35] Hoven C. V., Wang H., Elbing M., Garner L., Winkelhaus D., Bazan G. C., Chemically fixed p-n heterojunctions for polymer electronics by means of covalent B-F bond formation, *Nat. Mater.*, 9 (3), 249-252, 2010.
- [36] Kahraman G., Beşkardeş O., Rzayev Z. M. O., Pişkin E., Bioengineering polyfunctional copolymers. VII. Synthesis and characterization of copolymers of p-vinylphenyl boronic acid with maleic and citraconic anhydrides and their self-assembled macrobranched supramolecular architectures, *Polymer*, 45 (17), 5813-5828, 2004.
- [37] Kahraman G., Türk M., Rzayev Z. M. O., Ünsal M. E., Söylemez E., Bioengineering functional copolymers. XV. Synthesis of organoboron amide-ester branched derivatives of oligo(maleic anhydride) and their interaction with HeLa and L929 fibroblast cells. Collection of Czechoslovak Chemical Communications, *Collect Czech. Chem. C.*, 76 (8), 1013-1031, 2011.
- [38] Kataoka K., Miyazaki H., Okano T., Sakurai Y., Sensitive Glucose-Induced Change of the Lower Critical Solution Temperature of Poly[N,Ndimethylacrylamide-co-3-(acrylamido)phenylboronic acid] in Physiological Saline, *Macromolecules*, 27, 1061-1062, 1994.
- [39] Kersey F. R., Zhang G. Q., Palmer G. M., Dewhirst M. W., Fraser C. L., Stereocomplexed PLA-PEG nanoparticles with dual-emissive boron dyes for tumor accumulation, *ACS Nano*, 4 (9), 4989-4996, 2010.
- [40] Kishi N., Ahn C. H., Jin J., Uozumi T., Sano T., Soga K., Synthesis of polymer supported borate cocatalysts and their application to metallocene polymerizations, *Polymer*, 41 (11), 4005-4012, 2000.
- [41] Mager M., Becke S., Windisch H., Denninger U., Non-coordinating dendrimer polyanions: Cocatalysts for the metallocene-catalyzed olefin polymerization, *Angew. Chem., Int. Ed.*, 40 (10), 1898-1902, 2001.
- [42] Pfister A., Zhang G., Zareno J., Horwitz A. F., Fraser C. L., Phosphorescence in aqueous medium, *ACS Nano*, 2, 1252-1258, 2008.
- [43] Qin Y., Sukul V., Pagakos D., Cui C., Jakle F., Preparation of organoboron block copolymers via ATRP of silicon and boron-functionalized monomers, *Macromolecules*, 38, 8987-8990, 2005.
- [44] Roy D., Cambre J. N., Sumerlin B. S., Sugar-responsive block copolymers by direct RAFT polymerization of unprotected boronic acid monomers, *Chem. Commun.*, 21, 2477-2479, 2008.
- [45] Roy D., Cambre J. N., Sumerlin B. S., Triply-responsive boronic acid block copolymers: solution self-assembly induced by changes in temperature, pH, or sugar concentration, *Chem. Commun.*, 16, 2106-2108, 2009.
- [46] Rzayev Z. M. O., Türk M., Kahraman G., Pişkin E., Bioengineering functional copolymers. XIX. Synthesis of anhydride-organoboron functionalized copolymers and their interaction with cancer cells, *Hacettepe J. Biol. & Chem.*, 39 (2), 111-132, 2011.
- [47] Türk M., Kahraman G., Khalilova S. A., Rzayev Z. M. O., Oguztüzün S., Bioengineering functional copolymers. XVII. Interaction of organoboron amide-ester branched derivatives of poly(acrylic acid) with cancer cells, *J. Cancer Ther.*, 2 (2), 266-275, 2011.
- [48] Türk M., Rzayev Z. M. O., Kurucu G., Bioengineering functional copolymers. XII. Interaction of boron-containing and PEO branched derivatives of poly(MA-alt-MVE) with HeLa cells, *Health*, 2 (1) 51-61, 2010.
- [49] Zhang G., Chen J., Payne S. J., Kooi S. E., Demas J. N., Fraser C. L., Multi-Emissive difluoroboron dibenzoylmethane polylactide exhibiting intense fluorescence and oxygen-sensitive room-temperature phosphorescence, *J. Am. Chem. Soc.*, 129 (29), 8942-8943, 2007.
- [50] Cicek H., Koçak G., Ceylan Ö., Bütün V., Synthesis and antibacterial activities of boronic acid-based recyclable spherical polymer brushes, *Macromol. Res.*, 27 (7), 640-648, 2019.
- [51] Ahmadi Y., Siddiqui M.T., Mohd Q., Haq R., Ahmad S., Synthesis and characterization of surface-active antimicrobial hyperbranched polyurethane coatings based on oleo-ethers of boric acid, *Arab. J. Chem.*, Available online 10 July 2018.
- [52] He P., Zhu H., Ma Y., Liu N., Niu X., Wei M., Pan J., Rational design and fabrication of surface molecularly imprinted polymers based on multi-boronic acid sites for selective capture glycoproteins, *Chem. Eng. J.*, 367, 55-63, 2019.
- [53] Hasabelnaby S., Goudah A., Agarwal H. K., Abd Alla M. S. M., Tjarks W., Synthesis, chemical and enzymatic hydrolysis, and aqueous solubility of amino acid ester prodrugs of 3-carboranyl thymidine analogs for boron neutron capture therapy of brain tumors, *Eur. J. Med. Chem.*, 55, 325-334, 2012.
- [54] Sumitani S., Oishi M., Nagasaki Y., Carborane confined nanoparticles for boron neutron capture therapy: Improved stability, blood circulation time and tumor accumulation, *React. Funct. Polym.*, 71 (7), 684-693, 2011.
- [55] Chen W., Mehta S. C., Lu D. R., Selective boron drug delivery to brain tumors for boron neutron capture therapy, *Adv. Drug Deliver. Rev.*, 26 (2-3), 231-247, 1997.
- [56] Morin C., The chemistry of boron analogues of biomolecules, *Tetrahedron*, 50 (44), 12521-12569, 1994.
- [57] Valliant J. F., Guenther K. J., King A. S., Morel P., Schaffer P., Sogbein O. O., Stephenson K. A., The medicinal chemistry of carboranes, *Coordin. Chem. Rev.*, 232 (1-2), 173-230, 2002.
- [58] Yang W., Gao S., Wang B., Boronic acid compounds as potential pharmaceutical agents, *Med. Res. Rev.*, 23 (3), 346-368, 2003.